Title

Electrical Maxwell demon and Szilard engine utilizing Johnson noise, measurement, logic and control

Authors and Affiliations

L.B. Kish
corresponding author
Department of Electrical and Computer Engineering, Texas A&M University - College Station, TX 77843-3128, USA

C.G. Granqvist
Department of Engineering Sciences, The Ångström Laboratory, Uppsala University, P.O. Box 534, SE-75121 Uppsala, Sweden

Abstract

We introduce a purely electrical version of Maxwell's demon which does not involve mechanically moving parts such as trapdoors, etc. It consists of a capacitor, resistors, amplifiers, logic circuitry, and electronically controlled switches and uses thermal noise in resistors (Johnson noise) to pump heat. The only types of energy of importance in this demon are electrical energy and heat. We also demonstrate an entirely electrical version of Szilard's engine, i.e., an information-controlled device that can produce work by employing thermal fluctuations. The only moving part is a piston that executes work, and the engine has purely electronic controls and it is free of the major weakness of the original Szilard engine in not requiring removal and repositioning the piston at the end of the cycle. For both devices, the energy dissipation in the memory and other binary informatics components are insignificant compared to the exponentially large energy dissipation in the analog part responsible for creating new information by measurement and decision. Nevertheless, the dissipation in the memory and informatics parts is sufficient to secure the Second Law of Thermodynamics.

1. Introduction

Heat engines [1] utilize temperature differences to produce work while "heat demons" [2-8] employ information about instantaneous amplitudes of thermal fluctuations and execute control to produce a temperature difference and/or work. There has been an upsurge of interest in "heat demons", as evidenced from an extensive recent literature [9-18]. Furthermore there is an old debate [8-14, 19-21] on the question whether the energy dissipation due to erasure of information in the memory is the fundamental process to save the Second Law of Thermodynamics, or if the generation of new information via measurement and decision [2,13] and control requirements [9] are more important.

This paper introduces new and improved types of demons: they are purely electrical systems which employ the thermal voltage noise (Johnson noise) of resistors in thermal equilibrium. One of the demons pumps heat (similarly to Maxwell's demon) and the other produces work (similarly to Szilard's engine). Their common characteristics is that nothing but electrical energies appear in the fluctuations, measurement, decision, control and memory parts of the demons, and that all of the energy loss is due to dissipative electrical transport. This situation is very different from that of earlier versions of Maxwell's demon and Szilard's engine wherein various forms of energies are (implicitly) employed in the various components. In the case of Maxwell's demon, for example, the detection of an approaching molecule and its velocity require photoelectronics-based sensing that includes laser light (photon energy), photodiodes, electrical signals and energy, and an electromechanical system to drive the trapdoor, as well as related kinetic and potential mechanical energies. Similarly, in Szilard's engine, detecting the location of the molecule, controlling the lever and repositioning the piston require photonic, electrical and mechanical energies and implies related forms of energy dissipation.

Complete evaluations of the various energy dissipation channels have not been performed in earlier work on Maxwell's demon and Szilard's engine, which may be associated with difficulties to assess the transfer of energies between their different forms. However our purely electrical demons, which are introduced in this paper, offer fundamental advantages and provide a convenient methodology for such analyses.

2. Electrical Maxwell demon utilizing Johnson noise and control

2.1 General description

The electrical Maxwell demon described below employs the Johnson noise of resistors as well as measurement, decision, logic operations and control for pumping heat. One should note that control systems in general contain units for making measurements, decision and executing control. Figure 1 shows an electrical Maxwell demon in its starting *Stage*-1 extracting energy from the resistor to the left. The switch is in position 1, and the Johnson noise current of the resistor yields voltage fluctuations $U(t)$ in the capacitor with variance

$$U_{eff}^2 = \left\langle U^2(t) \right\rangle = \frac{kT}{C} \tag{1}$$

in accordance with Boltzmann's energy equipartition theorem. It leads to a mean energy of $kT/2$ in the capacitor [1], where U_{eff} is the effective noise voltage (root mean square, RMS, voltage) on the capacitor C. This voltage fluctuation is a Gaussian process with exponential relaxation and correlation time (relaxation time) τ expressed as

$$\tau = RC , \tag{2}$$

where R is the resistance, and with an amplitude distribution function $g(U)$ given by

$$g(U) = \frac{1}{U_{eff}\sqrt{2\pi}} \exp\left[-\frac{U^2}{2U_{eff}^2}\right] . \tag{3}$$
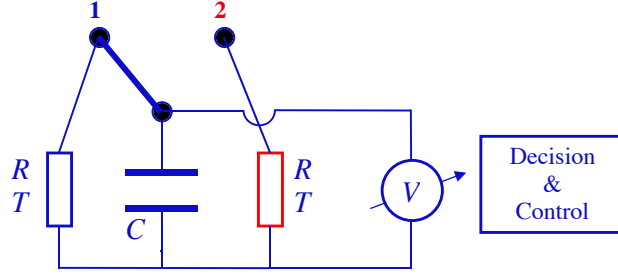
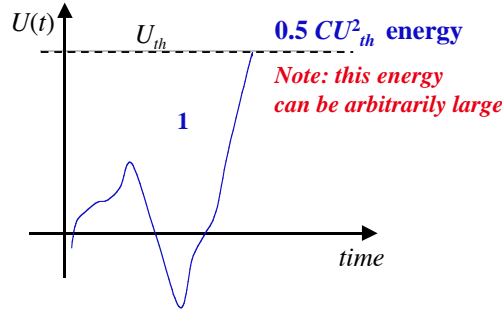Figure 1. Electrical Maxwell demon with Johnson noise in *Stage*-1.

Figure 2. Voltage fluctuations in the capacitor during *Stage*-1 for an electrical Maxwell demon with Johnson noise. (Note that real voltage fluctuations typically exhibit more "wiggles", as discussed later.)

The voltage $U(t)$ is monitored as illustrated in Figure 2, and the demon stays in *Stage*-1 until the voltage reaches a chosen arbitrary threshold value U_{th}, which corresponds to the energy

$$E_{th} = 0.5CU_{th}^2 \tag{4}$$

on the capacitor. The switch is then flipped to position 2, see Figure 3, and the demon gets into its *Stage*-2 wherein the capacitor is discharged and the energy E_{th} is pumped into the resistor on the right. In *Stage*-2, $U(t)$ is monitored on the capacitor, as shown in Figure 4, and when it reaches the zero threshold-level with $U(t) = 0$ the switch is flipped into its position 1 shown in Figure 1. Thus the demon gets into *Stage*-1 again and, through this step, the full cycle of the demon is completed.

By the end of *Stage*-1, the capacitor has extracted the energy $E_{th} = 0.5CU_{th}^2$ from the resistor on the left, and this energy is fully dissipated in the resistor on the right by the end of *Stage*-2. When the demon gets back to *Stage*-1 to start a new cycle, the energy in the capacitor is zero. Thus by the end of the new *Stage*-1 process, the capacitor again extracts $E_{th} = 0.5CU_{th}^2$ from the resistor on the left, and this energy will once more be fully dissipated in the resistor on the right by the end of the new *Stage*-2. Figure 5 illustrates voltage fluctuations during the whole cycle.
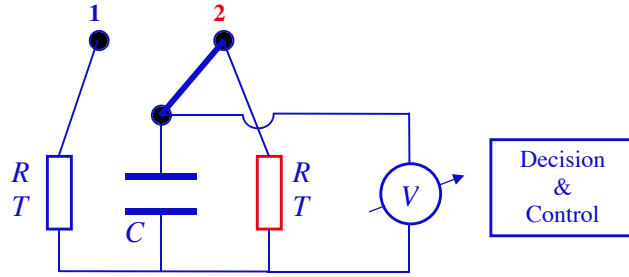
3

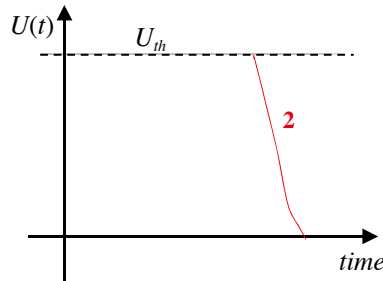Figure 3. Electrical Maxwell demon with Johnson noise in *Stage*-2.

Figure 4. Voltage fluctuations on the capacitor during *Stage*-2 for an electrical Maxwell demon with Johnson noise. (Note that real voltage fluctuations typically exhibit more "wiggles", as discussed later.)
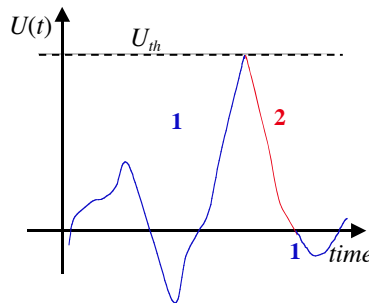

Figure 5. Voltage fluctuations in the capacitor, indicating the role of the two threshold levels U_{th} and 0 during the whole cycle, and the beginning of a new cycle.

It is important to note that, in an ideal system, the heat pumped during a single cycle does not have an upper limit because, according to Eq. 2, the threshold amplitude U_{th} (and thus the energy E_{th}) can be chosen to be arbitrarily large.

2.2. Cycle duration versus extracted heat/work during a cycle

The cycle frequency of Maxwell's demon is usually not part of its energy balance, but we note that an increase of the threshold U_{th} will cause an exponential slowdown of the demon as a result of the increased cycle time needed to reach U_{th}, as further discussed later. The duration of the exponential discharge process in *Stage*-2 scales logarithmically

4

with the pumped energy (threshold energy) E_{th}, whereas the duration of *Stage*-1 scales exponentially in the limit of large E_{th}, as discussed below. Thus the main question is the average duration of *Stage*-1, i.e., the mean first-passage time T_1 of the voltage fluctuation of the capacitor between zero and U_{th} when this energy is much greater than the average thermal energy in the capacitor; the threshold is given by

$$E_{th} = 0.5CU_{th}^2 >> 0.5kT . \tag{5}$$

This expression agrees with an earlier, analytic treatment of a Gaussian noise with exponential relaxation, where it was derived in an asymptotic limit [22].

A "dimensionless-first-passage-time" τ_1 from zero amplitude to the level U_{th} is given as

$$\tau_1(\eta) = \frac{\sqrt{\pi}}{2\eta} \exp\left(\eta^2\right) , \tag{6}$$

where $\tau_1(\eta) = T_1(\eta)/\tau$. Here η is the "dimensionless-threshold" T_1 and τ is the relaxation time of the Lorentzian. In our system, the dimensionless-threshold is $\eta = \frac{1}{\sqrt{2}} \frac{U_{th}}{U_{eff}}$, where $U_{eff} = \sqrt{kT/C}$ is the effective value of the noise. Thus the "real first-passage time" T_1 from zero amplitude to level U_{th} is

$$T_1(\zeta) = \tau_1(\eta)\tau = RC \frac{\sqrt{\pi}}{2\frac{1}{\sqrt{2}}\frac{U_{th}}{U_{eff}}} \exp\left(\frac{U_{th}^2}{2U_{eff}^2}\right) = RC\sqrt{\frac{\pi}{2}\frac{U_{eff}^2}{U_{th}^2}} \exp\left(\frac{U_{th}^2}{2U_{eff}^2}\right) =$$

$$= RC\sqrt{\frac{\pi}{2}\frac{kT}{CU_{th}^2}} \exp\left(\frac{CU_{th}^2/2}{kT}\right) = RC\sqrt{\pi\frac{kT}{4E_{th}}} \exp\left(\frac{E_{th}}{kT}\right) \propto RC\sqrt{\frac{kT}{E_{th}}} \exp\left(\frac{E_{th}}{kT}\right) . \tag{7}$$

In conclusion, even though an arbitrarily large energy E_{th} can be transferred by the Maxwell-demon-type heat pump within a cycle, the cycle duration scales exponentially with this energy, which means that increasing E_{th} results in an exponential scaling down of the mean power.

2.3. On energy requirement and dissipation

In this section, we discuss the energy dissipation in the limit of high threshold, $E_{th} >> kT$ (where Eq. 7 holds), and small error probability. A full assessment of the energy dissipation needed to run the demon requires consideration of all of its building elements. Such analyses have not been common in prior work, because the demon's *functional* characteristics have usually not been described in sufficient detail. To avoid mistakes caused by such deficiencies, Figure 6 shows the complete functional block scheme required to realize Maxwell's demon. A possible *physical realization* of this scheme is given in Figure 7.
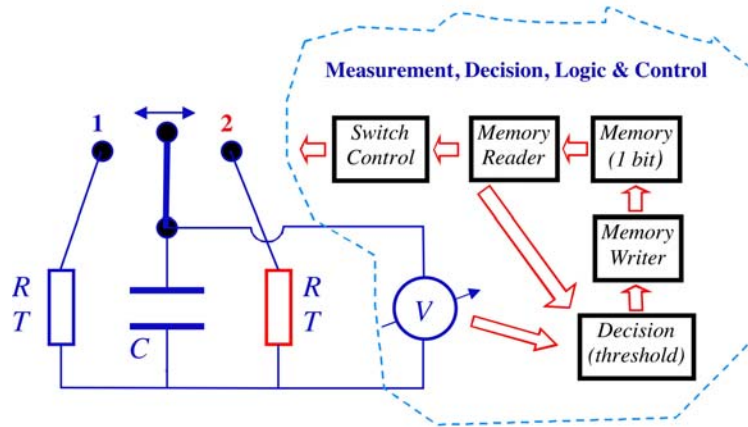
Figure 6. Electrical Maxwell demon showing the block scheme of the building elements for measurement, decision and control. The voltmeter and the threshold device create new information, and the rest of the system only processes/utilizes this binary information.
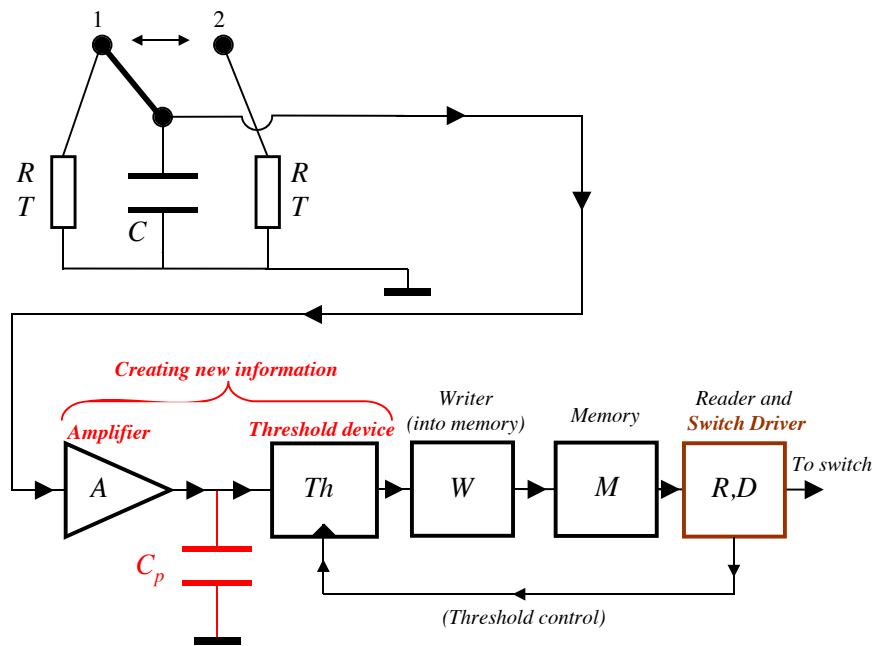

Figure 7. Possible realization of an electrical Maxwell demon. Some of these elements can be joined in other realizations, but the energy dissipation sources described here remain.

It is important to identify the dominant causes of energy dissipation. The first two stages of the *Measurement*, *Decision*, *Logic and Control* unit in Figure 6 are the *Amplifier* and the *Threshold device* in Fig. 7, which represent the measurement and decision. For example, the output of the *Threshold device* can be a positive or negative pulse representing the moment when the switch state must be changed from 1 to 2 or from 2 to 1 and triggering the *Memory* to alter its state accordingly. The *Memory* stores binary, single-bit information—a *High* or *Low* value—and these two-bit states signify the actual state (1 or 2) of the switch. During a single cycle of the demon, the single-bit information cycles through its two states *Low-High-Low* or *High-Low-High* depending on the choice

of the designer of the system: whether the *Low*-bit represents the switch-state 1 and the *High*-bit the switch-state-2, or *vice versa*.

The *Reader and Switch Driver* device is basically an amplifier system that reads out the memory status and checks the voltage-controlled switches, which either make a connection between the capacitor and point 1 while breaking the former connection to point 2, or *vice versa*. Thus these are two electronically controlled switches—between the capacitor and 1 and between the capacitor and 2, respectively—driven in alternate fashion.

We now consider the elements for handling the binary information and note that—according to Brillouin's negentropy principle [6,7]—the processing of each bit of information will dissipate energy of at least $kT \ln(2)$, and processing with acceptable error probability $(<< 0.5)$ will require even greater energy dissipation E_d [9,23]. Within the correlation time (reciprocal bandwidth) of thermal fluctuations, and in the small-error probability limit [9,23], the lower boundary of energy dissipation can be described by the Rice formula [23]. The required energy is logarithmically divergent when the error probability goes to zero according to

$$E_{d,bin} \approx kT \ln\left(\frac{1}{\varepsilon}\right) \quad \left[\text{Joule/bit}\right] , \tag{8}$$

where $\varepsilon << 0.5$ is the bit-error probability during the correlation time τ. Demanding the same numerical value of the error probability [9] for a longer cycle time (or clock period) $T_c >> \tau$ makes the energy dissipation increase logarithmically as a result of the additivity of independent errors generated in different non-overlapping correlation time intervals. It follows that

$$E_{d,bin} \approx kT \ln\left(\frac{1}{\varepsilon_c}\frac{T_c}{\tau}\right) \quad \left[\text{Joule/bit}\right] , \tag{9}$$

where $\varepsilon_c < 0.5$ is the bit-error probability during T_c. Using the result of Eq. 7, we obtain the following relation for the lowest possible energy dissipation of each binary switching element (transistor, etc) in the demon:

$$E_{d,bin} \geq kT \ln\left[\frac{1}{\varepsilon_c}\sqrt{\frac{kT}{E_{th}}}\exp\left(\frac{E_{th}}{kT}\right)\right] = E_{th} + kT\left[\ln\left(\frac{1}{\varepsilon_c}\sqrt{\frac{kT}{E_{th}}}\right)\right] . \tag{10}$$

We conclude that the Second Law of Thermodynamics is satisfied by even a single binary unit (such as any logic gate, or the memory) for the case of a fixed E_{th}/kT ratio and error probability approaching zero. The energy dissipation scales roughly with the energy threshold E_{th}, i.e., in the small error limit it scales with the pumped energy.

Turning now to the major sources of energy dissipation, we consider the *Amplifier* and the *Threshold-device*, which are the analog circuitry elements where new information is created. Their energy dissipation scale exponentially with E_{th} and is much larger than the amount required by the Second Law of Thermodynamics. Theoretically, if the chosen threshold level U_{th} is large enough, the *Amplifier* is not needed and it is sufficient with a

Threshold-device. However, any such device can be modeled as an amplifier with either saturation and/or positive feedback, and thus we keep the *Amplifier* stage because it helps us illustrate the point where the energy dissipation scales exponentially with E_{th}.

In order to elucidate the origin of the amplifier's energy dissipation, it should be realized that any amplifier has a component of *inertia*. To choose a simple illustrative example, a hydraulic amplifier has inertia due to the mass of its components. In the present case of an electrical voltage amplifier, inertia ensues from parasitic capacitances and inductances. We illustrate this issue of electrical inertia by considering the final capacitor, positioned at the point where the *Threshold-device* makes the decision about the threshold crossing, denoted C_p in Figure 7. For the sake of simplicity, we assume that the amplification is unity in the *Amplifier*. Under thermal equilibrium, thermal voltage fluctuations (Johnson noise) appear on the capacitor with an RMS value of $\sqrt{kT/C_p}$, which corresponds to a mean thermal energy of $kT/2$ in the capacitor. If this Johnson noise is not actively damped, then it must be kept at a much lower level than the main Johnson noise of the demon we are monitoring, i.e., $\sqrt{kT/C} \gg \sqrt{kT/C_p}$. This means that $C_p \gg C$ in order to reduce erroneous threshold crossings caused by the parasitic noise. We note, in passing, that it can be shown that active damping of the parasitic Johnson noise would cause greater energy dissipation than the value we discuss below [24].
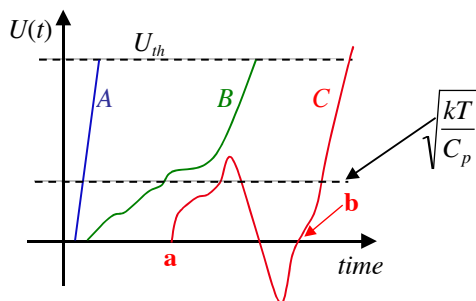

Figure 8. Illustration of the main source of energy dissipation in the electrical Maxwell demon. An exponential number of "voltage wiggles" as a function of the threshold energy take place before reaching the threshold. The energy dissipation between the points **a** and **b** represent complete energy loss and do not contribute to the process of attaining the threshold.

Figure 8 illustrates three possible trajectories of the voltage within *Stage*-1 as its amplitude goes from zero to U_{th}. Curves **A** and **B** represent monotonically increasing functions which reach U_{th} with relatively modest energy investment, i.e., $0.5 C_p U_{th}^2 \gg kT/2$ plus the thermalization losses due to the resistances, etc (not shown in the circuitry). However, curve **C** is qualitatively different and non-monotonic. This feature causes serious additional energy dissipation and, for example, all of the energy invested in the trajectory from points **a** to **b** is completely lost. For example, in the case of a symmetric power supply (i.e., with electrodes: +, –, and zero (ground)) the parts of the trajectory with positive velocity (increasing amplitude) are supplied by the positive electrode of the power source, while the decreasing parts of the trajectory are supplied by

8

the negative electrode, when in both cases the current flows into the ground. Both of these currents represent positive power extracted from the positive and negative parts of the supply, respectively. Even though a net energy was dissipated in the voltage-path from **a** to **b**, the whole charging process is back to zero at **b,** and all of the earlier invested energy was lost.

How many such dissipative "voltage wiggles" will the fluctuations in the capacitors exhibit, and how large are these fluctuations? During the correlation time $\tau = RC$ of the noise in the main capacitor, the noise typically goes through at least one large wave ranging though the +/– RMS amplitude interval. This means that the related energy dissipation E_{d1} during the correlation time of the main noise is of the order

$$E_{d1,an} \approx \frac{C_p}{C} kT \ .$$
(11)

According to Eq. 7, the expected number of correlation time (τ) periods during the dominant *Stage*-1 part of the clock cycle is $\sqrt{\frac{kT}{E_{th}}} \exp\left(\frac{E_{th}}{kT}\right)$, and hence the total energy dissipation is of the order

$$E_{d,an} \approx \frac{C_p}{C} kT \sqrt{\frac{kT}{E_{th}}} \exp\left(\frac{E_{th}}{kT}\right) \propto kT \exp\left(\frac{E_{th}}{kT}\right) \ .$$
(12)

Thus the dominant energy dissipation during a single cycle in the large-threshold energy limit is

$$E_{d,tot} > E_{d,an} + E_{d,bin} \approx \frac{C_p}{C} kT \sqrt{\frac{kT}{E_{th}}} \exp\left(\frac{E_{th}}{kT}\right) + E_{th} + kT \left[\ln\left(\frac{1}{\varepsilon_c}\sqrt{\frac{kT}{E_{th}}}\right)\right],$$
(13)

and hence the approximate scaling in this limit is

$$E_{d,tot} \propto kT \exp\left(\frac{E_{th}}{kT}\right) \ .$$
(14)

In conclusion, the dominant energy dissipation in the electrical Maxwell demon takes place in the part which generates the new information and is due its analog processing yielding an exponential dependence of the number of random voltage oscillations during a single cycle.

3. Electrical Szilard engine utilizing Johnson noise and control

The principles of the Johnson-noise-driven electrical Szilard engine are the same as those of the electrical Maxwell demon, though heat is not pumped but work is executed by a moving capacitor plate used as a piston [1]. The control and all other considerations are inherently the same as for Maxwell's demon, except the fact that the Szilard engine requires a twice as large system as the Maxwell demon. Thus two single-bit memories are needed, and the related voltage monitoring and switch control must be performed over two capacitors.

Figure 9 shows the main elements and circuitry of the electrical Szilard engine except the decision, logic and control components which are identical to the corresponding parts in Maxwell's demon. The electrical Szilard engine extracts heat from the resistor and executes work on the piston, which is the moving joint capacitor plate of the two capacitors at the middle.
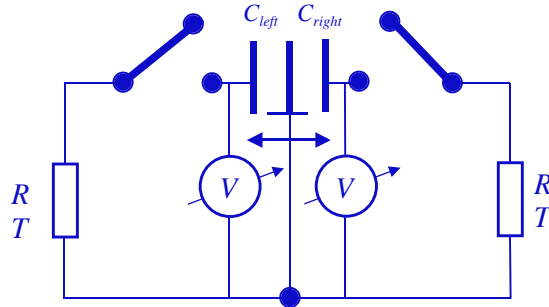

Figure 9. Electrical Szilard engine extracting heat from the resistor and executing work on the piston, i.e., the movable capacitor plate.

The left capacitor has its maximum capacitance $C_{left} = C_{max}$ when the piston is at the left end, while the right capacitor then attains its minimum capacitance $C_{right} = C_{min}$. In the opposite case, when the piston is at the right end, the left capacitor reaches its minimum value $C_{left} = C_{min}$ while the right capacitor has its maximum capacitance $C_{right} = C_{max}$. The capacitor with the minimum capacitance will be charged up to the work charge Q_w at different points of the cycle; they correspond to a threshold voltage $U_{th} = Q_w / C_{min}$, as shown in Figure 2. The corresponding electrical charging energy—analogously to the case of Maxwell's demon—is much greater than the thermal equilibrium value, i.e.,

$$E_w = 0.5 Q_{min}^2 / C >> kT/2 \ . \tag{15}$$

Figure 10(a) shows an arbitrarily chosen starting point of the cycle. The piston is at the right end and the capacitor to the right has the work charge Q_w. The voltage on the right capacitor is Q_w / C_{max}. The energy difference, compared to the situation with the opposite position of the piston at the same charge, is

$$-\Delta E = 0.5 Q_w \left(\frac{1}{C_{max}} - \frac{1}{C_{min}} \right) < 0 \ , \tag{16}$$

implying that the piston has a negative potential energy and sits in a potential well. We suppose that

$$\Delta E = 0.5 Q_w \left(\frac{1}{C_{min}} - \frac{1}{C_{max}} \right) >> kT/2 \ , \tag{17}$$

i.e., the piston remains at the bottom of this potential barrier, which is in the vicinity of the right end, while it executes its mechanical Brownian motion.
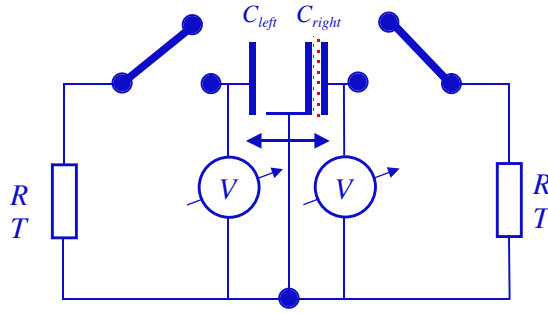
Figure 10. Arbitrarily chosen starting point of the cycle for the electrical Szilard engine. The piston is at the right end and the capacitor at the right has the work charge Q_w. The corresponding electrical energy is $E_w \gg kT/2$.

Figure 11 illustrates the operation of the first half-cycle for the electrical Szilard engine. In Figure 11(a), the left switch is closed in order to charge the left capacitor, and the Johnson noise current of the left resistor yields charge fluctuations in the left capacitor, which is a Gaussian noise of the charge; see Fig. 10(b). After an exponentially long waiting time characterized by Eq. 7, the left capacitor, which originally had zero charge, is charged up to the working charge Q_w and energy E_w given by Eq. 15. At that moment, the left switch is abruptly opened to keep the charge in the left capacitor, and the right switch is closed to discharge the capacitor on the right as shown in Fig. 10(c). The charge in the right capacitor decays exponentially and, within a time interval of a few RC, thermalizes and crosses the zero charge (zero voltage) level; see Fig. 10(d). At that moment, as illustrated in Fig. 10(e), the right switch is abruptly opened, and the zero charge (zero voltage) state is preserved in the right capacitor. Then the electrostatic force due to the working charge in the left capacitor moves the piston to the left end, as shown in Fig. 10(f), while, in accordance with the energy conservation law, the piston executes positive work amounting to ΔE. This is the end of the half-cycle. The piston is at the left end and the capacitor at the left has the work charge Q_w.

(a)
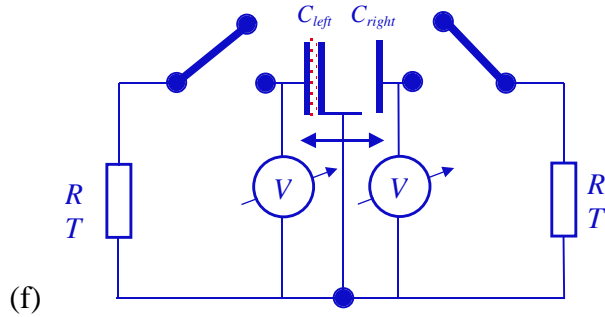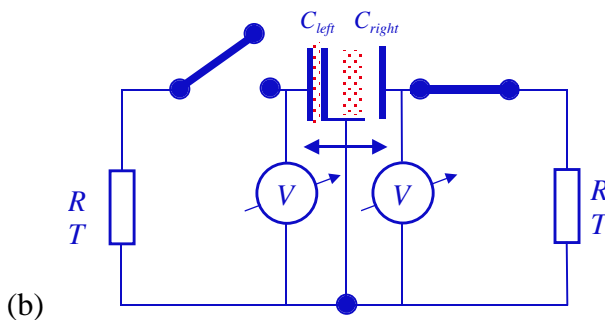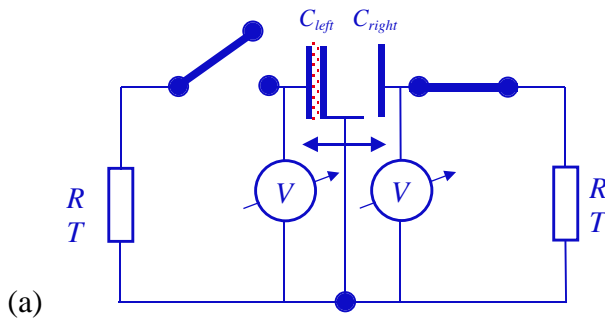
11

(b)

(c)

(d)

(e)

12

(f)
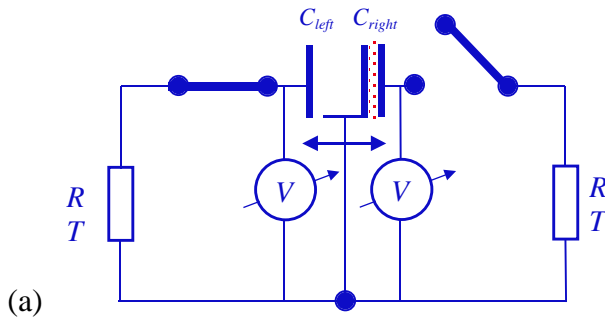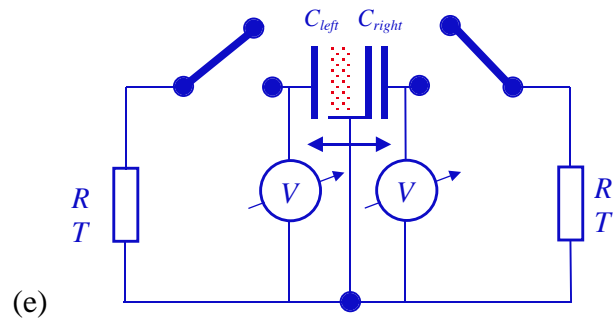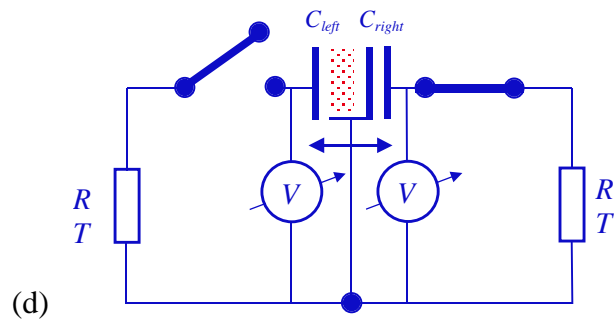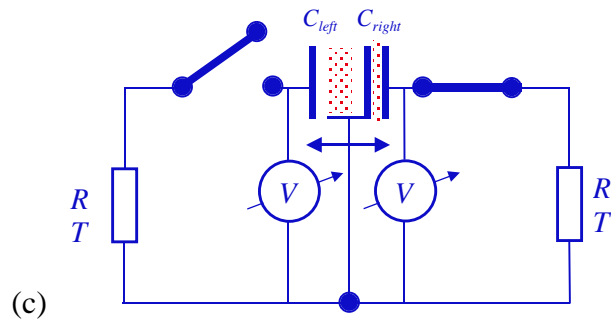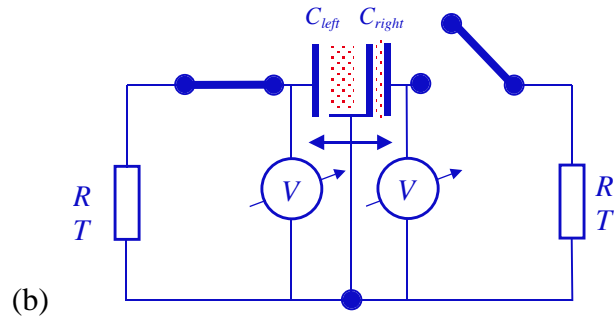
Figure 11. Operation of the first half cycle for the electrical Szilard engine. **(a):** The left switch is closed to charge the left capacitor. **(b):** Johnson noise current yields charge fluctuations in the left capacitor, i.e., a Gaussian noise in the charge. **(c):** As soon as the left capacitor reaches Q_w, the left switch is abruptly opened to keep the charge in the left capacitor and the right switch is closed to discharge the capacitor on the right. **(d):** The charge in the right capacitor decays exponentially and, within a time interval of a few RC, thermalizes and crosses the zero charge (zero voltage) level. **(e):** The right switch is abruptly opened and the zero charge (zero voltage) state is preserved in the right capacitor. **(f):** The force due to the working charge in the left capacitor moves the piston to the left end, which is the end of the half-cycle; the piston is at the left end and the capacitor at the left has the work charge Q_w.

The remainder of the full cycle comprises the same processes as during the first half, with the proper change of the indices signifying "left" and "right" of capacitors and switches, as elucidated in Figure 12.
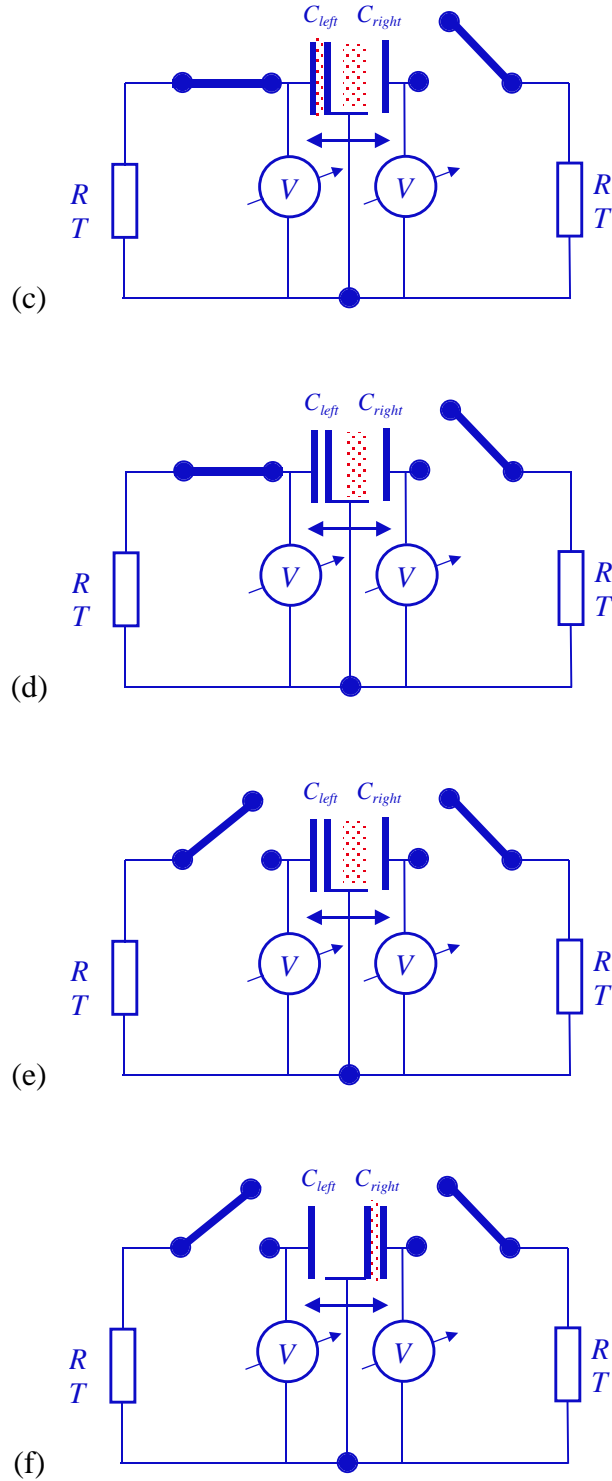

(a)

(b)

Figure 12. Operation of the second half cycle for the electrical Szilard engine. **(a):** The right switch is closed to charge the right capacitor. **(b):** Johnson noise current yields charge fluctuations in the right capacitor, i.e., a Gaussian noise in the charge. **(c):** As soon as the right capacitor reaches Q_w, the right switch is abruptly opened to keep the charge in the right capacitor and the left switch is closed to discharge the capacitor on the right. **(d):** The charge in the left capacitor decays exponentially and, within a time

14

interval of a few *RC*, thermalizes and crosses the zero charge (zero voltage) level. **(e):** The left switch is abruptly opened and the zero charge (zero voltage) state is preserved in the left capacitor. **(f):** The force due to the working charge in the right capacitor moves the piston to the right end, which is the end of the full cycle and the same state as where the analysis started; see Figure 10. The piston is at the right end and the capacitor in the right has the work charge Q_w.

Thus, the full cycle has been carried out with purely electronic control based on the information from the measurement of charge or voltage in the capacitors. It should be noted that the system is free from the major deficiency of the original Szilard engine, which is that its piston must be artificially relocated into the initial position at the end of the cycle. Because the two switches represent four possible states and two bits of information, the measurement-decision-logic-control unit is basically twice that of the system shown for the electrical Maxwell demon, while the energy dissipation essentially doubles. Thus the energy dissipation in the binary part, including in the memory, is negligible compared to that in the analog part that executes the measurement and creates the new information.

4. Conclusion

Two electrical demons utilizing Johnson noise, measurement, decision, logic and control were introduced; they are new versions of Maxwell's demon and Szilard's engine. We showed all of the necessary building elements and analyzed the cycle time versus the energy output. Both demons have an arbitrarily large energy output during a single cycle, and the cycle duration and energy dissipation scale exponentially with this energy output. The exponentially scaling energy dissipation occurs in the analog parts of the demons, where the creation of new information (measurement and decision) takes place. In the binary part, including the memory, the energy dissipation scales only linearly with the energy output, and even this dissipation is enough to satisfy the Second Law of Thermodynamics due to the enhanced energy threshold requirements caused by the exponentially long cycle duration and the requirement of keeping the error probability small.

Acknowledgments

References

[1]   Kish LB (2011) Thermal noise engines. Chaos Solitons Fractals 44:114–121.
[2]   Szilard L (1929) On the reduction of entropy in a thermodynamic system by the interference of an intelligent being. Z Phys 53:840–856.
[3]   Maxwell JC (1871) Theory of Heat. London: Longmans, Green & Co.

[4]   Leff HS, Rex AS (editors) (2003) Maxwell's Demon 2: Entropy, Classical and Quantum Information, Computing. Bristol: Institute of Physics.

[5]   Chialvo DR, Millonas MM (1995). Asymmetric unbiased fluctuations are sufficient for the operation of a correlation ratchet. Phys Lett A 209:26–30.

[6]   Brillouin L (1964) Scientific Uncertainty and Information. New York: Academic.

[7]   Brillouin L (1962) Science and Information Theory. New York: Academic.

[8]   Zurek WH (1986) Maxwell's demon, Szilard's engine and quantum measurements. In: Moore GT, Scully MO (editors). Proceedings of Frontiers of Non-Equilibrium Quantum Statistical Mechanics. New York: Plenum. pp. 145–150.

[9]   Kish LB, Granqvist CG (2012) Energy requirement of control: Comments on Szilard's engine and Maxwell's demon. EPL 98:68001.

[10] Norton JD (2011) Waiting for Landauer. Stud Hist Philos Mod Phys 42: 184–198.

[11] Norton JD (2005) Eaters of the lotus: Landauer's principle and the return of Maxwell's demon. Stud Hist Philos Mod Phys 36:375–411.

[12] Norton JD (2012) The end of the thermodynamics of computation: A no go result. (manuscript, to appear in Philosophy of Science). Available at http://www.pitt.edu/~jdnorton/papers/No_Go.pdf.

[13] Granger L, Kantz H (2011) Thermodynamic cost of measurements. Phys Rev E 84:061110.

[14] Gea-Banacloche J, Leff HS (2005). Quantum version of the Szilard one-atom engine and the cost of raising energy barriers. Fluct Noise Lett 5:C39–C47.

[15] Horowitz J, Parrondo JMR (2011) Designing optimal discrete-feedback thermodynamic engines. New J Phys 13:123019.

[16] Sagawa T, Ueda M (2012) Nonequilibrium thermodynamics of feedback control. Phys Rev E 85:031114.

[17] Vaikuntanathan S, Jarzynski C (2011) Modeling Maxwell's demon with a microcanonical Szilard engine. Phys Rev E 83:061120.

[18] Van den Broeck C (2010) Thermodynamics of information: Bits for less or more for bits? Nature Phys 6:937–938.

[19] Porod W (1988) Energy requirements in communication – Comment. Appl Phys Lett 52:2191–2191.

[20] Porod W, Grondin RO, Ferry DK (1984) Dissipation in computation. Phys Rev Lett 52:232–235.

[21] Porod W, Grondin RO, Ferry DK, Porod G (1984) Dissipation in computation – Reply. Phys Rev Lett 52:1206–1206.

[22] Lindenberg K, Seshadri V (1979) Analytic theory of extrema. I. Asymptotic theory for Fokker-Planck processes. J Chem Phys 71:4075–4084.

[23] Kish LB (2004) Moore's law and the energy requirement of computing versus performance. IEE Proc – Circuits Devices Systems 151 (2004) 190–194.

[24] Kish LB, Granqvist CG (2011) Energy requirement of control: Comments on Maxwell's demon and Szilard's engine. In: Alfinito E, Leuzzi M, Millithaler J-F (editors). All the Colors of Noise: Essays in Honor of Lino Reggiani. Cormigliano del Brenta: Munari Edizione. pp. 43–50.